DATASHEET

UF3SC065030B7S

650V-27mΩ SiC FET

Rev. B, May 2023

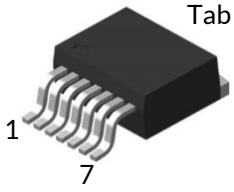

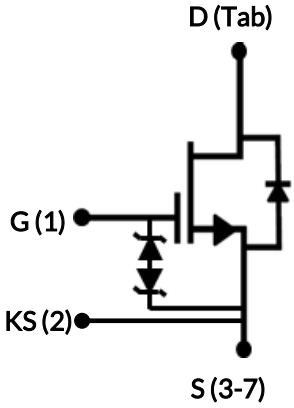

Part Number	Package	Marking
UF3SC065030B7S	D²PAK-7L	UF3SC065030B7S

Description

This SiC FET device is based on a unique 'cascode' circuit configuration, in which a normally-on SiC JFET is co-packaged with a Si MOSFET to produce a normally-off SiC FET device. The device's standard gate-drive characteristics allows for a true "drop-in replacement" to Si IGBTs, Si FETs, SiC MOSFETs or Si superjunction devices. Available in the D²PAK-7L package, this device exhibits ultra-low gate charge and exceptional reverse recovery characteristics, making it ideal for switching inductive loads , and any application requiring standard gate drive.

Features

- On-resistance $R_{DS(on)}$: 27mΩ (typ)
- Operating temperature: 175°C (max)
- Excellent reverse recovery: Q_{rr} = 425nC
- Low body diode V_{FSD}: 1.3V
- Low gate charge: Q_G = 43nC
- Threshold voltage $V_{G(th)}$: 5V (typ) allowing 0 to 15V drive
- Package creepage and clearance distance > 6.1mm
- Kelvin source pin for optimized switching performance
- ESD protected, HBM class 2

Typical applications

Any controlled environment such as

- Telecom and Server Power
- Industrial power supplies
- Power factor correction modules
- Motor drives
- Induction heating

Maximum Ratings

Parameter	Symbol	Test Conditions	Value	Units
Drain-source voltage	V_{DS}		650	V
Gate-source voltage	V_{GS}	DC	-25 to +25	V
Continuous drain current [1]	I_D	T_C = 25°C	62	A
		T_C = 100°C	44	A
Pulsed drain current [2]	I_{DM}	T_C = 25°C	230	A
Single pulsed avalanche energy [3]	E_{AS}	L=15mH, I_{AS} =4A	120	mJ
Power dissipation	P_{tot}	T_C = 25°C	214	W
Maximum junction temperature	$T_{J,max}$		175	°C
Operating and storage temperature	T_J, T_{STG}		-55 to 175	°C
Reflow soldering temperature	T_{solder}	reflow MSL 3	245	°C

1. Limited by $T_{J,max}$
2. Pulse width t_p limited by $T_{J,max}$
3. Starting T_J = 25°C

Thermal Characteristics

Parameter	Symbol	Test Conditions	Value			Units
			Min	Typ	Max	
Thermal resistance, junction-to-case	$R_{\theta JC}$			0.54	0.7	°C/W

Electrical Characteristics (T_J = +25°C unless otherwise specified)

Typical Performance - Static

Parameter	Symbol	Test Conditions	Value			Units
			Min	Typ	Max	
Drain-source breakdown voltage	BV_{DS}	V_{GS}=0V, I_D=1mA	650			V
Total drain leakage current	I_{DSS}	V_{DS}=650V, V_{GS}=0V, T_J=25°C		6	150	µA
		V_{DS}=650V, V_{GS}=0V, T_J=175°C		30		
Total gate leakage current	I_{GSS}	V_{DS}=0V, T_J=25°C, V_{GS}=-20V / +20V		6	± 20	µA
Drain-source on-resistance	$R_{DS(on)}$	V_{GS}=12V, I_D=40A, T_J=25°C		27	35	mΩ
		V_{GS}=12V, I_D=40A, T_J=125°C		36		
		V_{GS}=12V, I_D=40A, T_J=175°C		43		
Gate threshold voltage	$V_{G(th)}$	V_{DS}=5V, I_D=10mA	4	5	6	V
Gate resistance	R_G	f=1MHz, open drain		4.5		Ω

Typical Performance - Reverse Diode

Parameter	Symbol	Test Conditions	Value			Units
			Min	Typ	Max	
Diode continuous forward current [1]	I_S	T_C=25°C			62	A
Diode pulse current [2]	$I_{S,pulse}$	T_C=25°C			230	A
Forward voltage	V_{FSD}	V_{GS}=0V, I_S=20A, T_J=25°C		1.3	1.4	V
		V_{GS}=0V, I_S=20A, T_J=175°C		1.35		
Reverse recovery charge	Q_{rr}	V_R=400V, I_S=50A, V_{GS}=-5V, R_{G_EXT}=10Ω di/dt=2650A/µs, T_J=25°C		425		nC
Reverse recovery time	t_{rr}			25		ns
Reverse recovery charge	Q_{rr}	V_R=400V, I_S=50A, V_{GS}=-5V, R_{G_EXT}=10Ω di/dt=2650A/µs, T_J=150°C		280		nC
Reverse recovery time	t_{rr}			20		ns

Typical Performance - Dynamic

Parameter	Symbol	Test Conditions	Value			Units
			Min	Typ	Max	
Input capacitance	C_{iss}	V_{DS}=100V, V_{GS}=0V f=100kHz		1500		pF
Output capacitance	C_{oss}			320		
Reverse transfer capacitance	C_{rss}			2.3		
Effective output capacitance, energy related	$C_{oss(er)}$	V_{DS}=0V to 400V, V_{GS}=0V		230		pF
Effective output capacitance, time related	$C_{oss(tr)}$	V_{DS}=0V to 400V, V_{GS}=0V		520		pF
C_{OSS} stored energy	E_{oss}	V_{DS}=400V, V_{GS}=0V		18.5		µJ
Total gate charge	Q_G	V_{DS}=400V, I_D=40A, V_{GS} = -5V to 12V		43		nC
Gate-drain charge	Q_{GD}			11		
Gate-source charge	Q_{GS}			19		
Turn-on delay time	$t_{d(on)}$	V_{DS}=400V, I_D=40A, Gate Driver =-5V to +12V, Turn-on $R_{G,EXT}$=8.5Ω, Turn-off $R_{G,EXT}$=22Ω Inductive Load, FWD: same device with V_{GS} = -5V, R_G = 22Ω, T_J=25°C		25		ns
Rise time	t_r			28		
Turn-off delay time	$t_{d(off)}$			45		
Fall time	t_f			11		
Turn-on energy	E_{ON}			334		µJ
Turn-off energy	E_{OFF}			90		
Total switching energy	E_{TOTAL}			424		
Turn-on delay time	$t_{d(on)}$	V_{DS}=400V, I_D=40A, Gate Driver =-5V to +12V, Turn-on $R_{G,EXT}$=8.5Ω, Turn-off $R_{G,EXT}$=22Ω Inductive Load, FWD: same device with V_{GS} = -5V, R_G = 22Ω, T_J=150°C		23		ns
Rise time	t_r			26		
Turn-off delay time	$t_{d(off)}$			46		
Fall time	t_f			9		
Turn-on energy	E_{ON}			308		µJ
Turn-off energy	E_{OFF}			75		
Total switching energy	E_{TOTAL}			383		

Typical Performance Diagrams

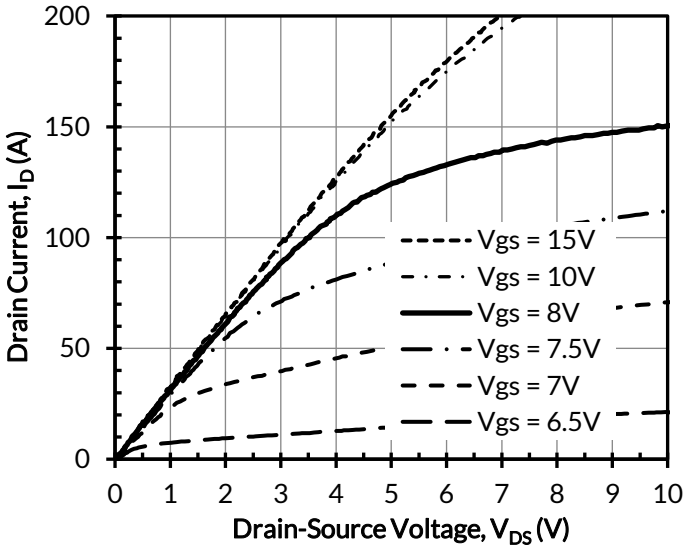

Figure 1. Typical output characteristics at T_J = - 55°C, tp < 250µs

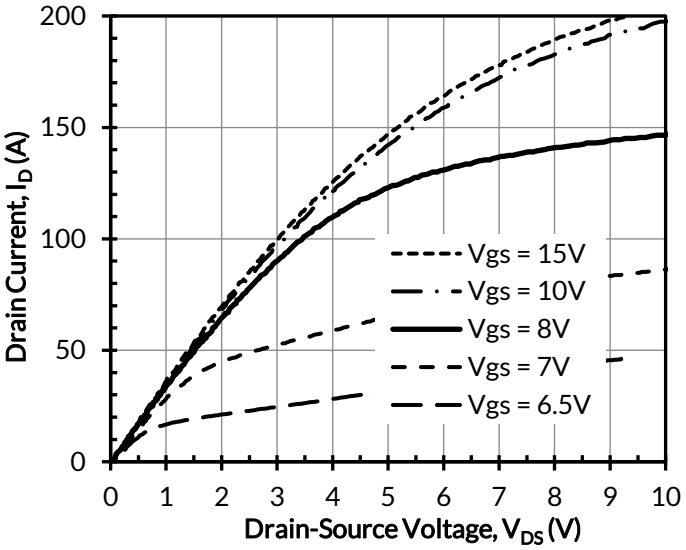

Figure 2. Typical output characteristics at T_J = 25°C, tp < 250µs

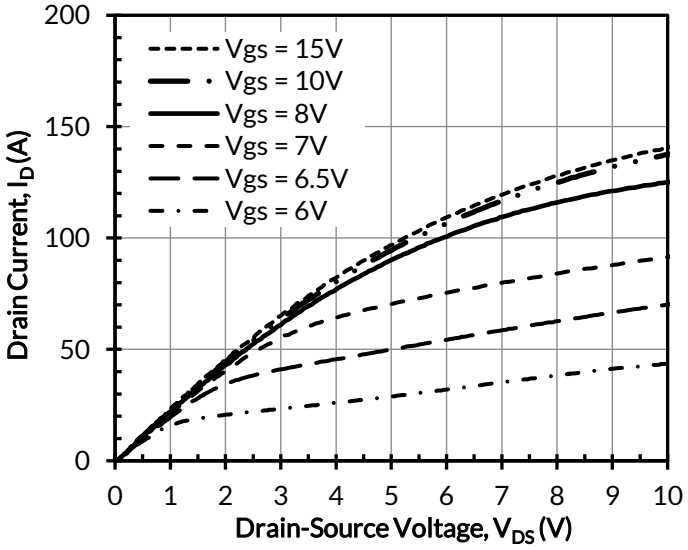

Figure 3. Typical output characteristics at T_J = 175°C, tp < 250µs

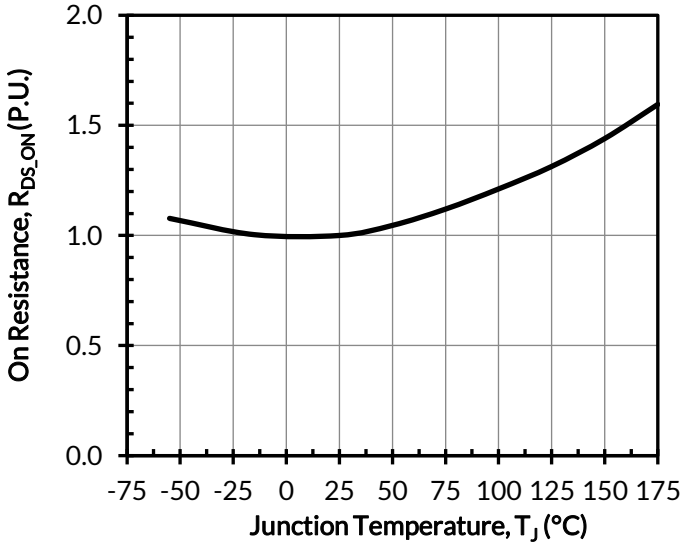

Figure 4. Normalized on-resistance vs. temperature at V_{GS} = 12V and I_D = 40A

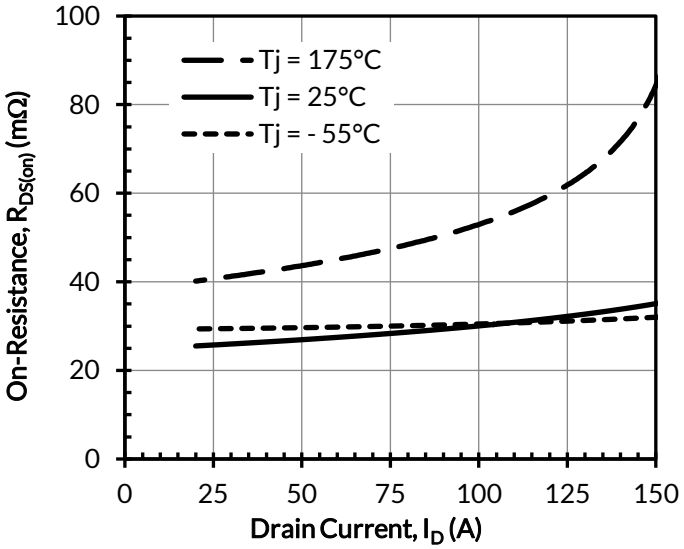

Figure 5. Typical drain-source on-resistances at V_{GS} = 12V

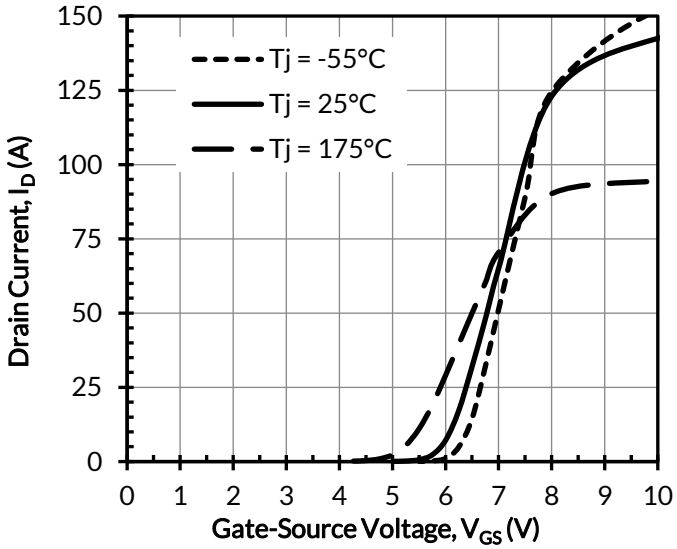

Figure 6. Typical transfer characteristics at V_{DS} = 5V

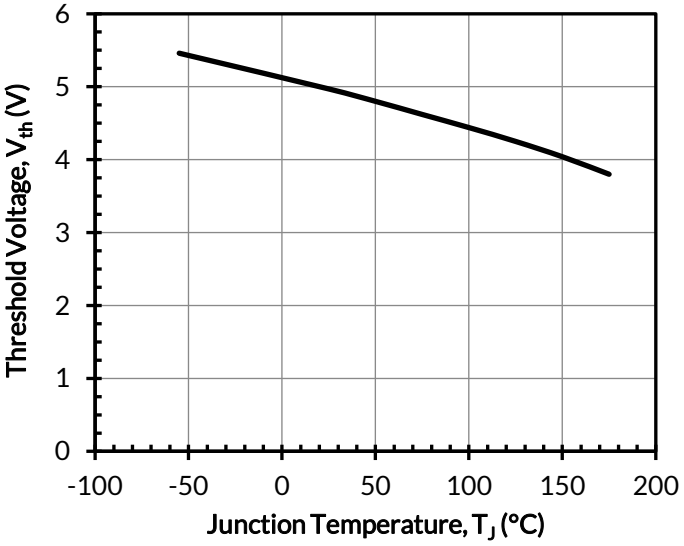

Figure 7. Threshold voltage vs. junction temperature at V_{DS} = 5V and I_D = 10mA

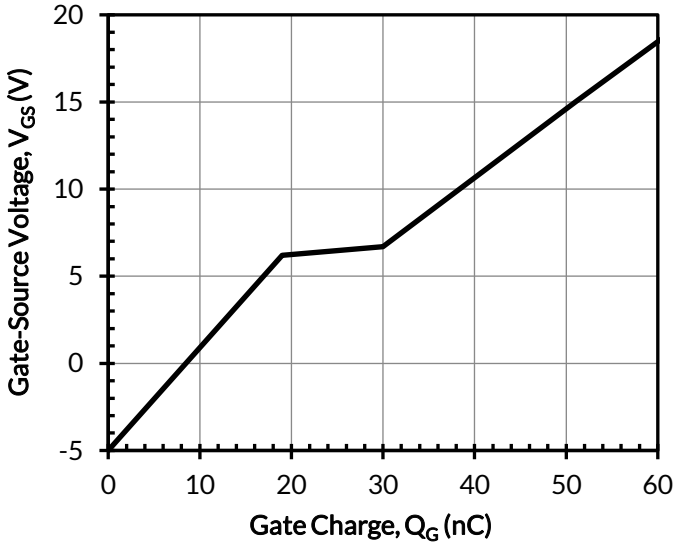

Figure 8. Typical gate charge at V_{DS} = 400V and I_D = 40A

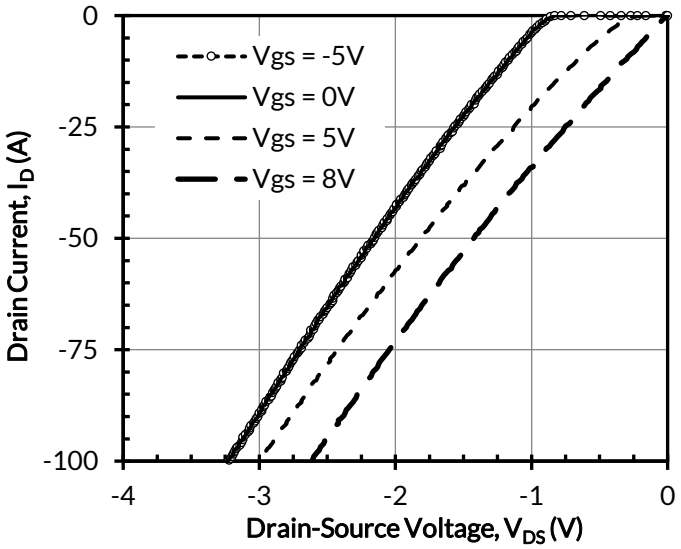

Figure 9. 3rd quadrant characteristics at T_J = -55°C

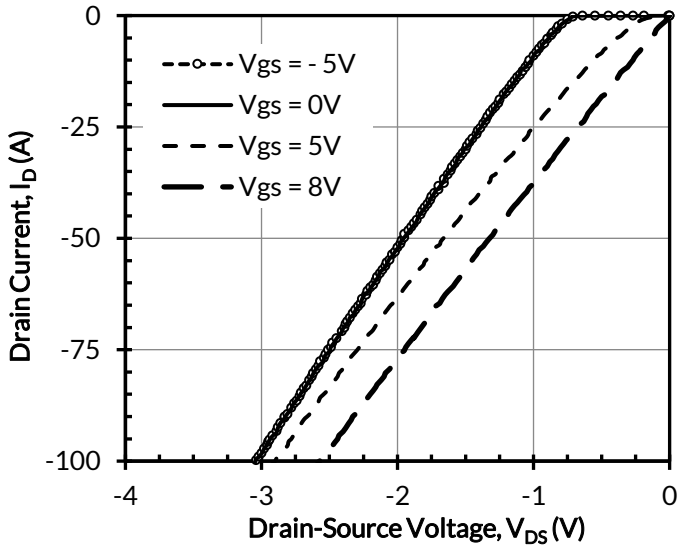

Figure 10. 3rd quadrant characteristics at T_J = 25°C

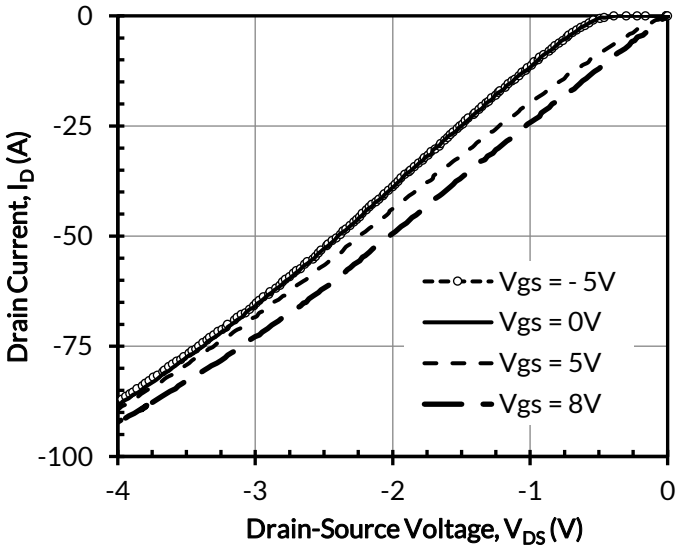

Figure 11. 3rd quadrant characteristics at T_J = 175°C

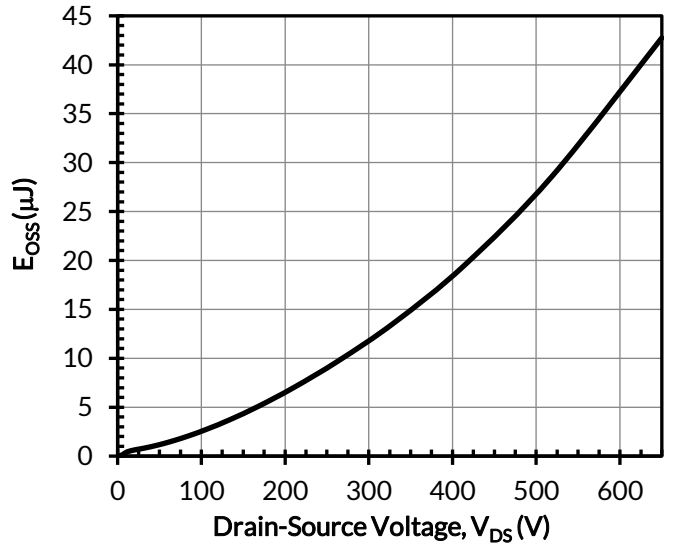

Figure 12. Typical stored energy in C_{OSS} at V_{GS} = 0V

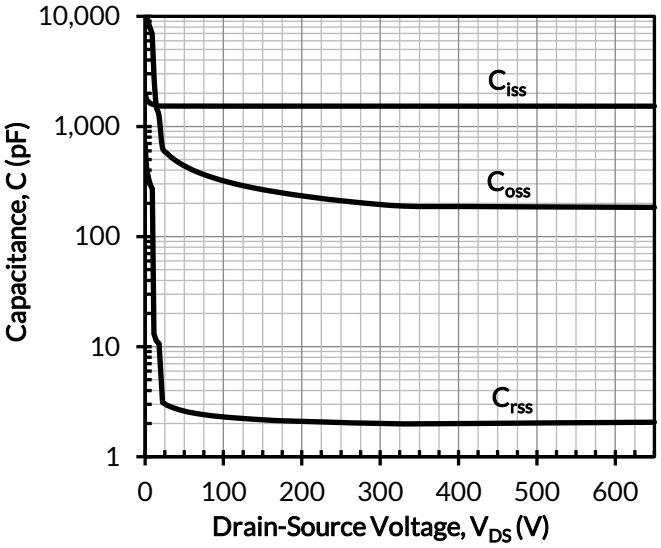

Figure 13. Typical capacitances at f = 100kHz and V_{GS} = 0V

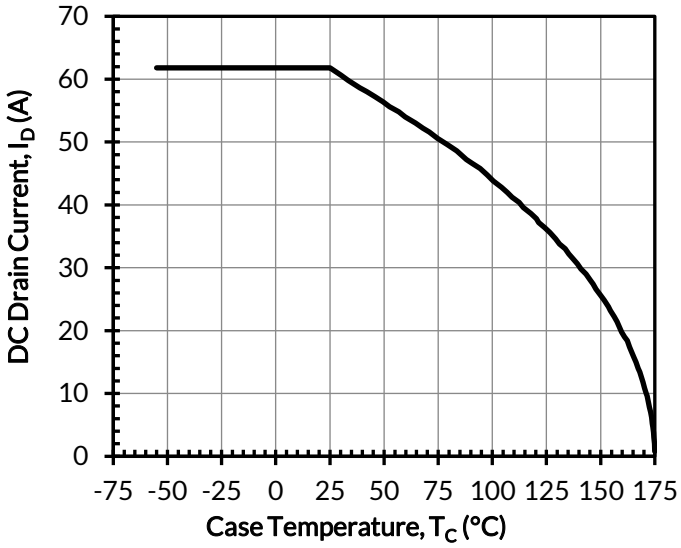

Figure 14. DC drain current derating

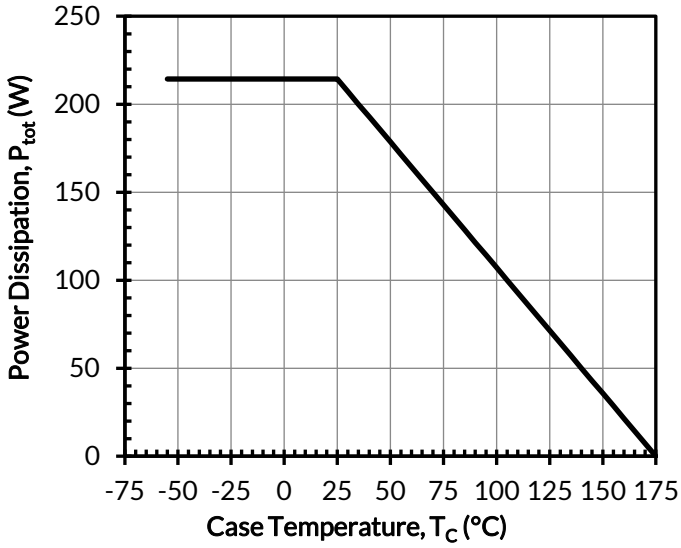

Figure 15. Total power dissipation

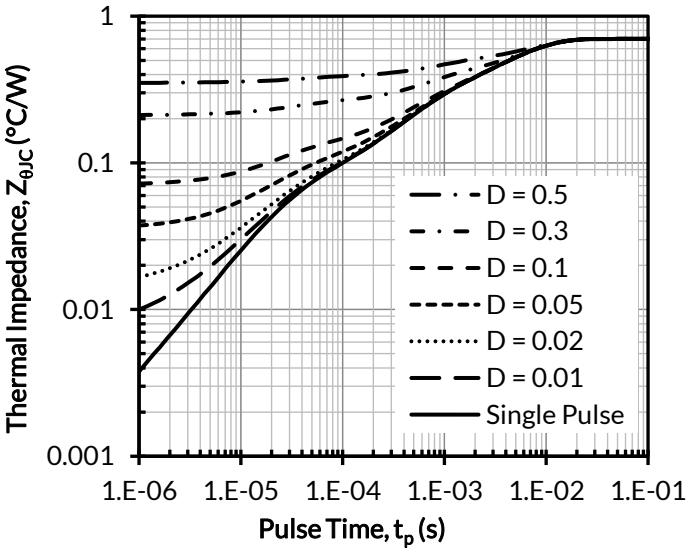

Figure 16. Maximum transient thermal impedance

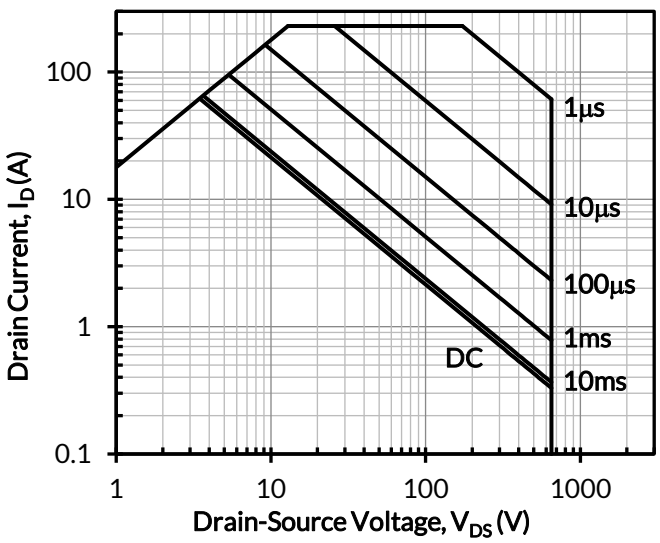

Figure 17. Safe operation area at T_C = 25°C, D = 0, Parameter t_p

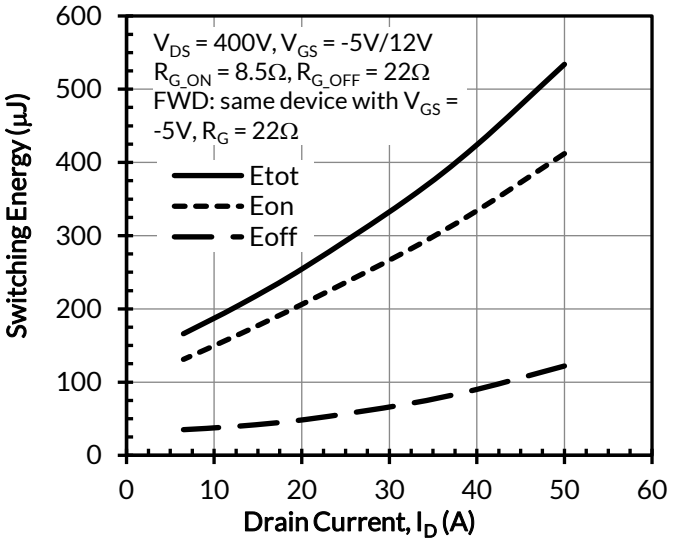

Figure 18. Clamped inductive switching energy vs. drain current at T_J = 25°C

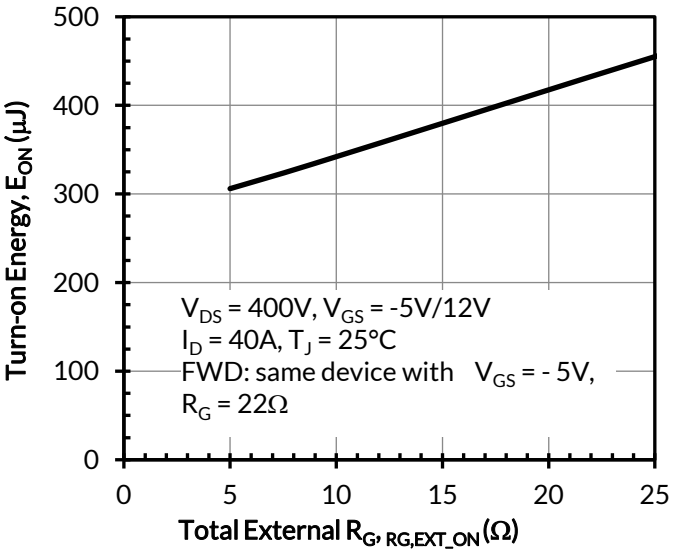

Figure 19. Clamped inductive switching turn-on energy vs. R_{G,EXT_ON}

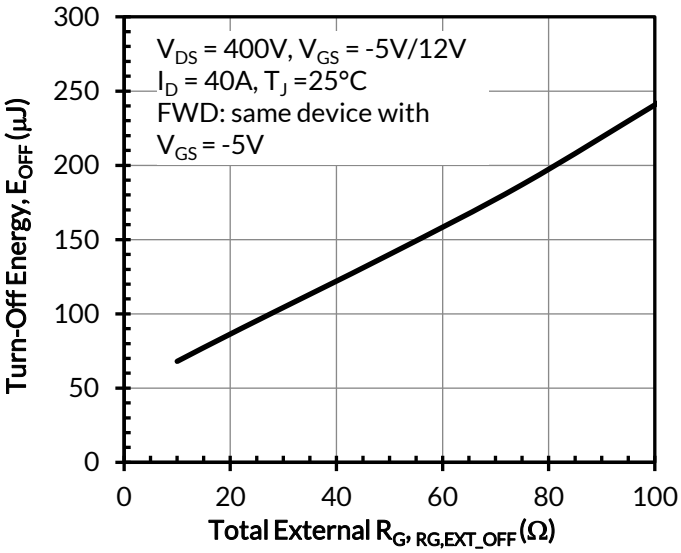

Figure 20. Clamped inductive switching turn-off energy vs. R_{G,EXT_OFF}

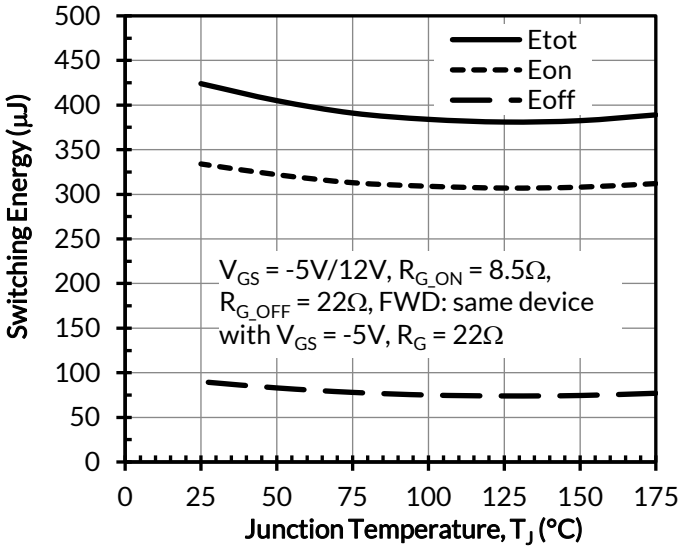

Figure 21. Clamped inductive switching energy vs. junction temperature at V_{DS} = 400V and I_D = 40A

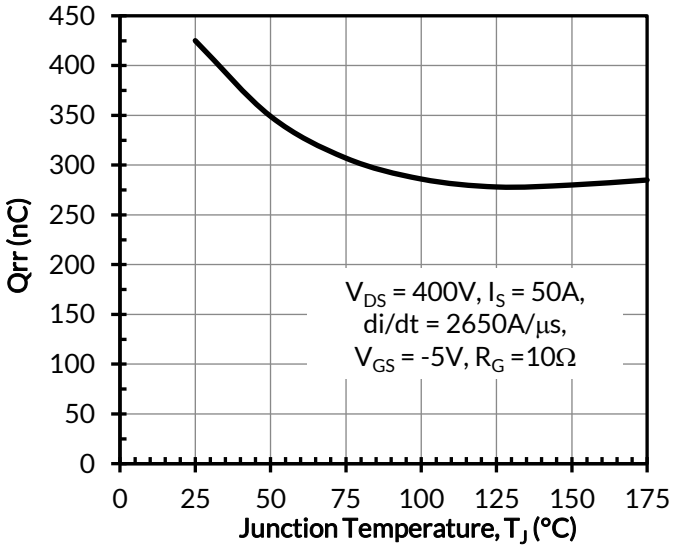

Figure 22. Reverse recovery charge Qrr vs. junction temperature

Applications Information

SiC FETs are enhancement-mode power switches formed by a high-voltage SiC depletion-mode JFET and a low-voltage silicon MOSFET connected in series. The silicon MOSFET serves as the control unit while the SiC JFET provides high voltage blocking in the off state. This combination of devices in a single package provides compatibility with standard gate drivers and offers superior performance in terms of low on-resistance ($R_{DS(on)}$), output capacitance (C_{oss}), gate charge (Q_G), and reverse recovery charge (Q_{rr}) leading to low conduction and switching losses. The SiC FETs also provide excellent reverse conduction capability eliminating the need for an external anti-parallel diode.

Like other high performance power switches, proper PCB layout design to minimize circuit parasitics is strongly recommended due to the high dv/dt and di/dt rates. An external gate resistor is recommended when the FET is working in the diode mode in order to achieve the optimum reverse recovery performance. For more information on SiC FET operation, see www.unitedsic.com.

A snubber circuit with a small $R_{(G)}$, or gate resistor, provides better EMI suppression with higher efficiency compared to using a high $R_{(G)}$ value. There is no extra gate delay time when using the snubber circuitry, and a small $R_{(G)}$ will better control both the turn-off $V_{(DS)}$ peak spike and ringing duration, while a high $R_{(G)}$ will damp the peak spike but result in a longer delay time. In addition, the total switching loss when using a snubber circuit is less than using high $R_{(G)}$, while greatly reducing $E_{(OFF)}$ from mid-to-full load range with only a small increase in $E_{(ON)}$. Efficiency will therefore improve with higher load current. For more information on how a snubber circuit will improve overall system performance, visit the UnitedSiC website at www.unitedsic.com

Important notice

The information contained herein is believed to be reliable; however, Qorvo makes no warranties regarding the information contained herein and assumes no responsibility or liability whatsoever for the use of the information contained herein. All information contained herein is subject to change without notice. Customers should obtain and verify the latest relevant information before placing orders for Qorvo products. The information contained herein or any use of such information does not grant, explicitly or implicitly, to any party any patent rights, licenses, or any other intellectual property rights, whether with regard to such information itself or anything described by such information. THIS INFORMATION DOES NOT CONSTITUTE A WARRANTY WITH RESPECT TO THE PRODUCTS DESCRIBED HEREIN, AND QORVO HEREBY DISCLAIMS ANY AND ALL WARRANTIES WITH RESPECT TO SUCH PRODUCTS WHETHER EXPRESS OR IMPLIED BY LAW, COURSE OF DEALING, COURSE OF PERFORMANCE, USAGE OF TRADE OR OTHERWISE, INCLUDING THE IMPLIED WARRANTIES OF MERCHANTABILITY AND FITNESS FOR A PARTICULAR PURPOSE. Without limiting the generality of the foregoing, Qorvo products are not warranted or authorized for use as critical components in medical, life-saving, or life-sustaining applications, or other applications where a failure would reasonably be expected to cause severe personal injury or death.